

# Class-level Multiple Distributions Representation are Necessary for Semantic Segmentation

Jianjian Yin<sup>1,2</sup> Zhichao Zheng<sup>2,3</sup> Yanhui Gu<sup>1,2</sup> Junsheng Zhou<sup>1,2</sup> Yi Chen<sup>1,2\*</sup>

<sup>2</sup>School of Computer and Electronic Information, Nanjing Normal University, China

<sup>1</sup>{212202015, gu, zhoujs, cs\_chenyi}@njnu.edu.cn <sup>3</sup>zheng\_zhichaoX@163.com

## Abstract

Existing approaches focus on using class-level features to improve semantic segmentation performance. How to characterize the relationships of intra-class pixels and inter-class pixels is the key to extract the discriminative representative class-level features. In this paper, we introduce for the first time to describe intra-class variations by multiple distributions. Then, multiple distributions representation learning (MDRL) is proposed to augment the pixel representations for semantic segmentation. Meanwhile, we design a class multiple distributions consistency strategy to construct discriminative multiple distribution representations of embedded pixels. Moreover, we put forward a multiple distribution semantic aggregation module to aggregate multiple distributions of the corresponding class to enhance pixel semantic information. Our approach can be seamlessly integrated into popular segmentation frameworks FCN/PSPNet/CCNet and achieve 5.61%/1.75%/0.75% mIoU improvements on ADE20K. Extensive experiments on the Cityscapes, ADE20K datasets have proved that our method can bring significant performance improvement.

## 1. Introduction

Semantic segmentation is a classical task in computer vision, aiming to assign semantic labels to each pixel in an image accurately. Semantic segmentation has extensive applications in the fields of autonomous driving, medical diagnosis and so on. In the last few years, the performance of semantic segmentation has improved tremendously with the development of deep neural network[15],[4]. Full convolutional network[27] based on encoder-decoder architecture becomes the cornerstone of all approaches. Existing methods generally focus on two problems to improve the performance of segmentation. One is how to change the structure of the network so as to improve

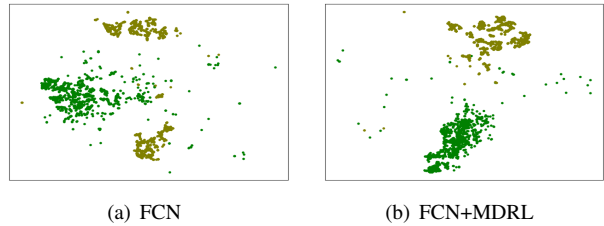


Figure 1: **t-SNE visualization on Cityscapes val.** We selected pixel features of the train(olive points) and road(green points) for tsne visualization.

the pixel feature representation[29],[6],[36],[5]. The other is to obtain contextual information to enhance the pixel representation[4],[11],[13],[16],[38],[42]. This paper investigates the same direction as the latter, with the aim of how to obtain richer contextual/semantic information to improve the performance of segmentation.

The methods obtaining contextual information are broadly divided into two types, multi-scale feature aggregation and relational contextual aggregation. For multi-scale feature aggregation, Deeplab[4] uses various dilation convolutions to capture contextual information at multiple scales. PSPNet[42] introduces pyramid spatial pooling to aggregate contextual information. For relational contextual aggregation, ACFNet[39] and OCRNet[37] divide pixels in an image into multiple regions and then increase the pixel representation by weighting the aggregated region representation, the weights are determined by the relationship between the pixels and the regions. Although the above methods are effective, they ignore the potential contextual information between the input images. In other words, there is no consideration of using class-level features beyond image to enhance the pixel representations.

In order to obtain class-level features beyond the input image, MCIBI[18] proposes to use simulated annealing to find a semantic feature on each class. Furthermore, MCIBI++[20] assuming that the class-level features satisfy a **Gaussian** distribution, the pixel representations are en-

\*Corresponding author.

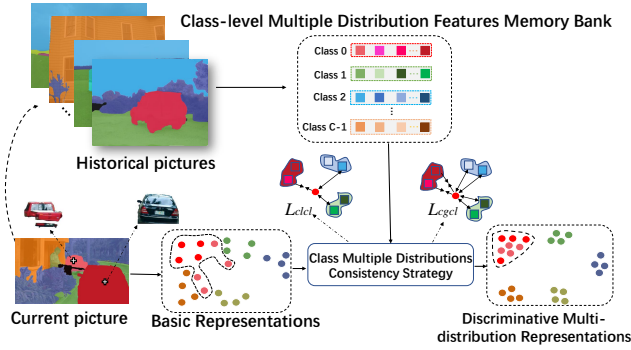


Figure 2: **Describe class representation by multiple distribution features.** The representation of cars with different colors are obviously different. Intra-class compact and inter-class dispersion are realized by class multiple distributions consistency strategy, which includes the class local consistency loss  $L_{clcl}$  and the class global consistency loss  $L_{cgcl}$ .

hanced by randomly generating the corresponding class feature by mean and variance each time. As shown in the Figure 1, we listed pixel features of two classes for tsne visualization, the result indicates that intra-class features have large divergence. MCIBI [18] and MCIBI++ [20] both use a feature or distribution to describe the representation of each class, which is not comprehensive.

In this paper, multiple distributions are introduced to describe intra-class divergence. We propose the multiple distributions representation learning (MDRL) to extract more semantic information per class, and augment the pixel representations. Meanwhile, we design the class multiple distributions consistency strategy, which contains the class local/global consistency loss. The class local consistency loss is to make pixels more compact with the nearest distribution of the same class and farther from the other classes nearest distribution. Class global consistency loss leverages multiple distribution features per class to achieve intra-class compactness and inter-class dispersion. Details can be seen in Figure 2. Several single distribution feature representations are obtained by feature voting based on the weights of the pixel representations and multiple distribution features for each class. Finally, a novel multiple distributions semantic aggregation module aggregates several single distribution feature representations to get the more fine-grained multiple distribution feature representations.

In a nutshell, our main contributions have four main points:

- To the best of our knowledge, this paper first explores multiple distributions to describe intra-class variations, resulting in richer class-level semantic features.
- We propose a class multiple distributions consistency strategy to construct discriminative multiple distribution

feature representations of embedded pixels.

- We put forward a novel multiple distributions semantic aggregation module to obtain more fine-grained multiple distribution feature representations, which is used to augment the pixel representations.

- We have done extensive experiments on different datasets and compared it with other state-of-the-art methods, the results show that our method can bring significant performance improvement.

## 2. Related Work

**Semantic Segmentation** Semantic segmentation methods based on FCN [27] have been very successful. Some studies [4], [44], [26] have targeted the refinement of the results generated by FCN. Specifically, these studies are broadly divided into two directions. One is to design more efficient network [36], [29], [41], [15] structures to extract more robust pixel feature representations, a backbone network called HRNet was designed by Wang [29], which maintains a high-resolution pixel representation during training. ResNet [15] proposes a residual structure to refine the features at each layer, resulting in a more robust pixel representation. The other is to obtain more contextual information [2], [11], [28], [42], [34], [4] to enhance the original pixel representations. The ways of capturing contextual information broadly include attention mechanisms [11], using different dilation rates [6] to increase the receptive field and building feature pyramids [21], [25]. In addition to this, the approach of taking care to balance the semantic features of classes when obtaining contextual information is proposed by [19]. The focus of this paper is on the latter, i.e., enhancing the pixel representations by aggregating multiple distribution features per class.

**Context Aggregation** Contextual information is extremely important for pixel-level classification tasks and is utilized in many research areas. The Deeplab [4], [5], [6] family proposes multiple atrous convolution rates to increase the perceptual field of the network and thus aggregate more contextual information. DenseASPP [34], developed based on the Deeplab, stitches the dilated rates in a densely connected manner to generate multi-scale features that not only cover a wider range but are also dense. PSPNet [42] adopts spatial pooling to obtain feature maps with different receptive field sizes. DANet [11] and OCNNet [38] calculate the pixel-to-pixel similarity as the weights, and weighted aggregation of all pixels to enhance the pixel representations. Apart from this, other methods [23], [37], [39] proposed to divide pixels into multiple regions and enhance the feature representations of pixel by computing the similarity between pixels and regions as weights for weighted aggregation. Although the above methods are effective, they only extract the contextual information of a single image. But in this paper, our approach learn class-level multiple distribu-

tions beyond input image to agument semantic information.

**Feature Memory Bank** The feature memory bank can store the effective class features during the neural network training. It has shown effectiveness in several computer vision work[7],[22],[30],[1],[32],[20],[18]. For instance, [30] explores the contrastive loss of pixels between different images by saving the class features of the pixels through the memory bank in several batches. [32] use the memory bank to save the features of negative samples of each class to make the features of the same class similar and the features of different classes more discriminative. The memory bank of the above methods store the class-level features generated by backbone. [18] uses feature memory bank to store the class-level features that generated by simulating annealing. [20] assumes that the class-level features satisfy a Gaussian distribution and store the mean and variance of each class by memory bank. In this paper, memory bank is utilized by us to store class-level multiple distribution features.

### 3. Methodology

In this section, we first introduce the overall flow of our method. Then describe the various parts involved in the method, including feature clustering, feature voting, multiple distributions semantic aggregation. Finally, we describe the details of class local consistency loss and class global consistency loss.

#### 3.1. Overview

Input an RGB image  $I \in \mathbb{R}^{3 \times H \times W}$ , mapping pixels to a non-linear embedding space through the backbone network  $N_t$  as follows:

$$R = N_t(I) \quad (1)$$

where the matrix  $R$  denotes the pixel representations of  $I$  with the size  $Z \times \frac{H}{8} \times \frac{W}{8}$ .  $Z$  stands for the number of channels. As shown in Figure 3, we generate a more fine-grained multiple distribution feature representation  $R_{dl}$  through the multiple distributions semantic aggregation module:

$$R_{dl} = DSA(R, \sum_{i=1}^N f_v(Weg, m_i)) \quad (2)$$

where  $m_i$  represents the  $i$ -th distribution feature of each class.  $Weg$  represents the class probability obtained after convolution and softmax of the feature map  $R$ .  $f_v()$  indicates the feature voting operation.  $N$  indicates the number of distributions of each class in the memory bank.  $DSA()$  represents multiple distributions semantic aggregation operation. The size of  $R_{dl}$  is  $Z \times \frac{H}{8} \times \frac{W}{8}$ .

Some methods[42],[4] have the ability to aggregate the semantic information of single image. In order to easily

integrate our method into existing method frameworks, we refer to the single image semantic aggregation as  $SSA$ . We can obtain the semantic features of single image:

$$R_{il} = SSA(R) \quad (3)$$

where  $R_{il}$  is the semantic information of the current image. Next, the pixel representation  $R$  are enhanced with multiple distribution feature representation  $R_{dl}$  and single image semantic feature representation  $R_{il}$  as follows:

$$R_{aug} = T(R, R_{il}, R_{dl}) \quad (4)$$

$T()$  is transform operator to fuse the basic representation  $R$ ,  $R_{il}$  and  $R_{dl}$ . Here it is important to note that  $R_{il}$  is optional. Finally, we need to classify the enhanced feature representation  $R_{aug}$  and upsample it to obtain the corresponding semantic segmentation probability distribution map:

$$O = UP_{8 \times}(cls(R_{aug})) \quad (5)$$

where  $cls()$  is a classification head and  $O$  is a matrix of  $C \times H \times W$ .  $C$  is the number of classes in the dataset.

#### 3.2. Feature Clustering

The purpose of clustering is to bring pixel features of the same class closer together and those of different classes further apart. Clustering creates a natural bottleneck[17] which discard the details of instance-specific features. Therefore, we choose multi-distribution features of each class as sub-center of the corresponding class.

Given the current batch of pixel  $P^c = \{p_m\}_{m=1}^M$  that belong to class  $c$ .  $M$  denotes the number of pixels. Our goal is to aggregate these pixels of the same class into  $N$  distributions  $\{d_{c,n}\}_{n=1}^N$ . We denote pixel-to-distribution mapping as  $L^c = [l_{p_m}]_{m=1}^M \in \{0, 1\}^{N \times M}$ , where  $l_{p_m} = [l_{p_m,n}]_{n=1}^N \in \{0, 1\}^N$  is the one-hot assignment vector of pixels  $p_m$  over the  $N$  distributions. Maximize the similarity between pixel embedding  $I^c = [p_m]_{m=1}^M \in \mathbb{R}^{G \times M}$  and distributions  $D^c = [d_{c,n}]_{n=1}^N \in \mathbb{R}^{G \times N}$  to optimize  $L^c$

$$\begin{aligned} \max_{L^c} & Tr(L^{c\top} D^{c\top} I^c) + \lambda \sum_{m,n} -l_{p_m,n} \log l_{p_m,n} \\ s.t. & L^c \in \mathbb{R}_+^{N \times M}, L^{c\top} \mathbf{1}^N = \mathbf{1}^M, L^c \mathbf{1}^M = \frac{M}{N} \mathbf{1}^N \end{aligned} \quad (6)$$

where  $\mathbf{1}^N$  represents a vector of  $N$  dimensions all 1.  $L^{c\top} \mathbf{1}^N = \mathbf{1}^M$  ensures that each pixel is assigned to a distribution.  $L^c \mathbf{1}^M = \frac{M}{N} \mathbf{1}^N$  enforces that each distribution is selected at least  $\frac{M}{N}$  times in the current batch[3].  $\lambda > 0$  is a parameter that controls the smoothness of distribution. The solution of Eq.6 can be given as[9]:

$$L^c = diag(u) exp\left(\frac{D^{c\top} I^c}{\lambda}\right) diag(v) \quad (7)$$

where  $u \in \mathbb{R}^N$  and  $v \in \mathbb{R}^M$  are renormalization vectors which computed by few steps of Sinkhorn-Knopp iteration[9].

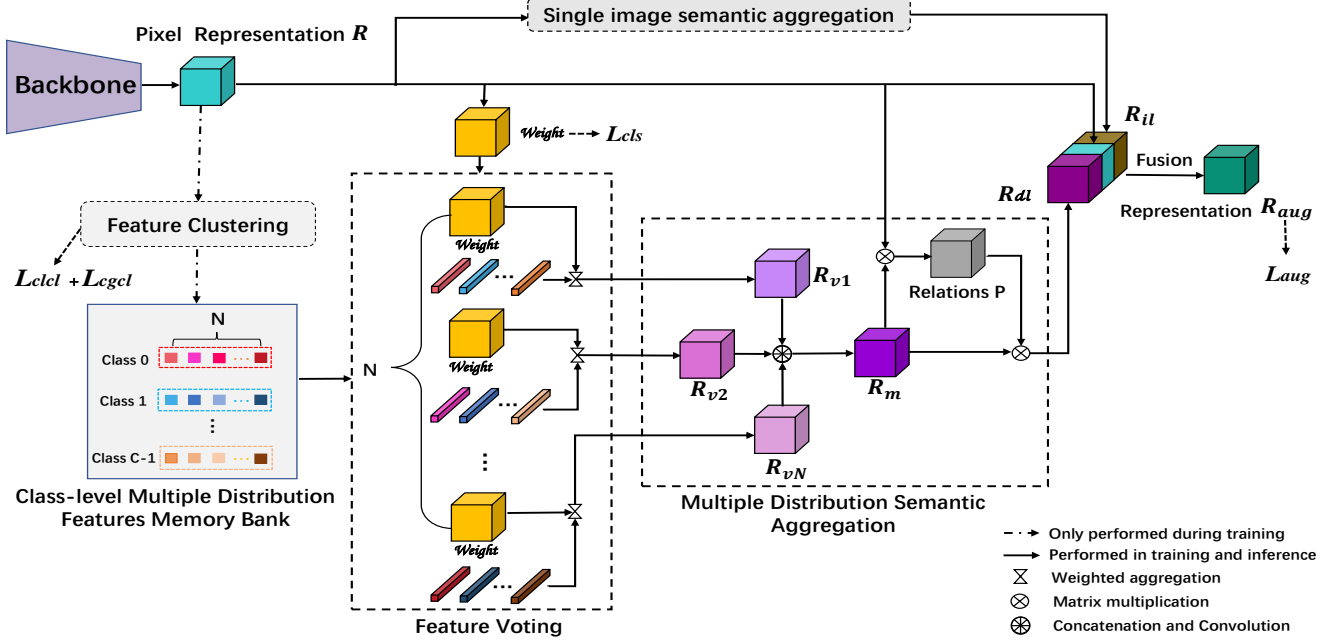


Figure 3: **Overview of multiple distributions representation learning.** The pixel representations  $R$  are clustered by the class multiple distributions consistency strategy to update the class-level multiple distribution features stored in memory bank. The single distribution feature representations  $R_{vi}$  generated by feature voting are aggregated by multiple distributions semantic aggregation module to obtain a fine-grained multiple distribution feature representation  $R_{dl}$ . Single image semantic aggregation is an optional operation that is specific to some existing methods (e.g., PPM[42],ASPP[4]).

**Feature Memory Update** For any distribution of each class in the memory bank, we choose pixels that closest to this distribution to update during each training iteration by following way:

$$d_{c,n} = \mu d_{c,n} + (1 - \mu) b_{c,n} \quad (8)$$

where  $b_{c,n}$  indicates the  $\ell_2$ -normalized vector of the embedded training pixels, which are closest to  $d_{c,n}$ . Here it is necessary to ensure that the class of the distribution is the same as the class of the pixels.  $\mu \in [0, 1]$  is a momentum update factor. Following[46],  $\mu$  is set to 0.999.

### 3.3. Feature Voting

Feature memory bank stores the class-level multiple distribution features  $\{\{d_{c,1}, d_{c,2}, \dots, d_{c,N}\}\}_{c=1}^C$ .  $D_i = \{d_{c,i}\}_{c=1}^C$  is the distribution feature of each class used for feature voting in  $i$ -th group. The basic feature representations  $R$  is convolved and softmax operated to obtain the weight matrix  $weight$ . Feature Voting is achieved by the following way:

$$R_{vi} = \text{resize}(\text{permute}(weight) \otimes D_i) \quad (9)$$

where  $\text{permute}(weight)$  is used to make  $weight$  have size of  $\frac{HW}{64} \times C$ , with the size of  $C \times Z$  for  $D_i$ .  $\otimes$  denotes for

the matrix multiplication.  $Z$  denotes the dimension of the distribution feature,  $\text{resize}()$  represents the conversion of the size to  $\frac{H}{8} \times \frac{W}{8} \times Z$ .

### 3.4. Multiple Distribution Semantic Aggregation

Several single distribution feature representations  $\{R_{vi}\}_{i=1}^N$  are obtained after feature voting. We fuse these representations to obtain the coarse multiple distribution feature representation  $R_m$ . Since the predicted result is obtained by  $R$  alone, pixels may be misclassified. To address this problem, we calculate the relations between  $R$  and  $R_m$  so that we can obtain a position confidence weight to further refine  $R_m$ . We calculate the relations  $P$  by the following equation:

$$P = \text{softmax}\left(\frac{g_a(\text{permute}(R)) \otimes g_b(R_m)^T}{\sqrt{\frac{C}{2}}}\right) \quad (10)$$

where  $\text{permute}()$  aims to change the size of  $R$  to  $\frac{HW}{64} \times C$ .  $R_m$  is refined by following equation:

$$R_{dl} = \text{rescale}(g_c(P \otimes g_f(R_m))) \quad (11)$$

where  $g_a, g_b, g_c$  and  $g_f$  change the number of channels per pixel,  $\text{rescale}()$  denotes to let the output have size of  $Z \times \frac{H}{8} \times \frac{W}{8}$ .

### 3.5. Loss Function

**Class local consistency loss** We use  $N$  distribution features  $\{d_{c,n}\}_{n=1}^N$  to characterize each class  $c \in \{1, \dots, C\}$ . In this way, the detailed features of each class can be captured by our method, the prediction of each pixel  $i \in I$  is realized by the following way:

$$\hat{c}_i = c^* \quad \text{with } (c^*, n^*) = \arg \min_{(c,n)} \{\langle i, d_{c,n} \rangle\}_{c,n=1}^{C,N} \quad (12)$$

where  $i \in \mathbb{R}^Z$  denotes the  $\ell_2$ -normalized embedding of pixel  $i$ .  $\langle \cdot, \cdot \rangle$  is the negative cosine similarity as distance measure, just as  $\langle i, d \rangle = -i^\top d$ . We define the class probability distribution of pixel  $i$  as:

$$p(c|i) = \frac{\exp(-s_{i,c})}{\sum_{cc=1}^C \exp(-s_{i,cc})} \quad (13)$$

where  $s_{i,c} = \min_{n=1}^N \{\langle i, d_{c,n} \rangle\}$ , represents the distance between the current pixel  $i$  and the nearest distribution chosen from the class to which it belongs. Given the ground-truth class of the current pixel  $i$ ,  $c_i \in \{1, \dots, C\}$ , The cross-entropy loss of the class local consistency:

$$L_{clcl} = -\log p(c_i|i) = -\log \frac{\exp(-s_{i,c_i})}{\exp(-s_{i,c_i}) + \sum_{cc \neq c_i} \exp(-s_{i,cc})} \quad (14)$$

The operation of the class local consistency loss lies in first filtering out a distribution feature of each class that is closest to the current pixel  $i$ . Eq.14 can be viewed as pushing pixel  $i$  closer to the nearest distribution feature of its corresponding class, and far away from other close distribution features of unrelated classes.

**Class global consistency loss** The class local consistency loss only utilize one distribution of each class. With the idea of fully using multi-distribution features of each class, we design the class global consistency loss to fulfill intra-class compactness and inter-class dispersion. Ablation experiment proves that the class global consistency loss and the class local consistency loss complement each other to better improve the segmentation performance.

For pixel  $i$ , class global consistency loss takes  $N$  distribution features of the true class as positive samples and  $(C-1) \times N$  distribution features of other unrelated classes as negative samples for contrastive loss. We define the class global consistency loss as:

$$L_{cgcl} = -\log \frac{A}{A+B} \quad (15)$$

$$A = \sum_{j=1}^N \exp(-\langle z_{ci}, z_{ci,j}^+ \rangle / \tau)$$

$$B = \sum_{jj=1}^{(C-1) \times N} \exp(-\langle z_{ci}, z_{ci,jj}^- \rangle / \tau)$$

where  $z_{ci}$  denotes the feature of pixel  $i$ ,  $z_{ci,j}^+$  represents the positive sample features of pixel  $i$ ,  $z_{ci,jj}^-$  denotes the negative sample features of pixel  $i$ . Following [24], the  $\tau$  is set to 0.5.

**Classification loss** There are two types of classification losses in our approach. One is for the loss of the basic feature representation  $R$  as:

$$L_{cls} = \frac{1}{H \times W} \sum_{(i,j)} L_{ce}(trans(R_{[* , i, j]}), GT_{[ij]}) \quad (16)$$

and the other is for the loss of the enhanced feature representation  $R_{aug}$  as:

$$L_{aug} = \frac{1}{H \times W} \sum_{(i,j)} L_{ce}(trans(R_{aug[* , i, j]}), GT_{[ij]}) \quad (17)$$

where  $L_{ce}$  represents the cross entropy loss,  $trans()$  denotes the transformation of the feature representation into a class probability distribution map.  $GT$  represents the ground-truth.

We optimize the overall loss as follows:

$$L = \eta L_{cls} + L_{aug} + \alpha L_{clcl} + \beta L_{cgcl} \quad (18)$$

Following [18], we set  $\eta$  as 0.4. We do detailed ablation experiments for weight  $\alpha$  and  $\beta$  of class local consistency loss and class global consistency loss respectively. We obtained the optimal weight after the ablation experiment, which set  $\alpha = 0.01$  and  $\beta = 0.05$ .

## 4. Experiments

### 4.1. Experimental Setup

**Datasets** We conduct experiments on two widely-used semantic segmentation benchmarks:

- Cityscapes**[8] is derived from urban scene. It has 5,000 finely annotated data with 19 classes. The dataset is divided into 2975/500/1525 for train/val/test.

- ADE20K**[45] is a large scene parsing dataset that includes 150 classes. The training, validation and test sets consists of 20K,2K,3K images, respectively.

**Training Settings** Our experiments are based on the PyTorch framework. The backbone networks adopt ResNet50 and ResNet101[15] which pretrained on ImageNet[10]. Color jitter, random scaling and horizontal flipping are used for data augmentation. We adopt SGD algorithm to optimize the network parameters, learning rate is updated by poly strategy with factor  $(1 - \frac{\text{iter}}{\text{max.iter}})^{0.9}$ . The detailed training settings on each dataset are listed as follows:

- Cityscapes:** The initial learning rate adjusted as 0.01, with weight decay is set to 0.0005. The input size of the image for the neural network is 512×1024, training epochs and batch size are set as 220 and 8, respectively.

- ADE20K:** We set the initial learning rate as 0.01, with weight decay is set to 0.0005. We crop the image size to 512×512 as the input to the network, batch size as 16 and training epochs as 130.

**Inference Settings** For the inference, we set the batch size to 1, the input image size is the same as the original image, but note that we also need multi-distribution features of each class for enhanced basic representations during the inference.

**Evaluation Metrics** The standard mean intersection-over-union(mIoU) is used by us to measure the performance of the algorithm.

**Reproducibility** Our approach is based on pytorch(version=1.10.0), trained on eight NVIDIA 3090 GPUs with a 24 GB memory per-card and two NVIDIA A40 GPUs with a 48 GB memory per-card. And all the testing procedures are performed on a NVIDIA A40 GPU.

## 4.2. Ablation Study

**Integrated into popular segmentation frameworks.** As illustrated in Table 1, we can see that our approach has greatly improved the performance of the popular network(FCN, PSPNet, CCNet). For instance, our approach brings 4%/5.61% mIoU improvements to FCN framework on Cityscapes/ADE20K. And for stronger frameworks PSPNet/CCNet, the performance can get about 1.5%/0.63% mIoU improvements on Cityscapes and 1.75%/0.75% mIoU improvements on ADE20K. Experimental results demonstrate that our approach not only can integrates seamlessly into popular frameworks, but also delivers a high level of improvement.

Method	Backbone	Stride	Cityscapes	ADE20K
FCN[27]	ResNet-50	×8	75.16	36.96
+ours	ResNet-50	×8	<b>79.16</b>	<b>42.57</b>
PSPNet[42]	ResNet-50	×8	78.55	42.64
+ours	ResNet-50	×8	<b>80.05</b>	<b>44.39</b>
CCNet[16]	ResNet-50	×8	79.15	42.47
+ours	ResNet-50	×8	<b>79.78</b>	<b>43.22</b>

Table 1: **The improvement when combining our approach with popular frameworks.** All the results are based on a single-scale validation.

**Number of class distributions** As illustrated in Table 2, different number of distributions can cause large different results. The divergence in performance between using 7 distributions and 9 distributions per class is close to 1.69% mIoU. Meanwhile, the results illustrate that it is necessary to use multiple distribution features to characterize the class representation, rather than just one. In other experiments, we used 9 distribution features to describe the intra-class variations.

**Validity of class local/global consistency loss** We verified the two losses separately. As illustrated in Table 3, using class local consistency loss alone can result in 3.04% mIoU

Method	Backbone	Dataset	num	mIoU
FCN[27]	ResNet-50	Cityscapes	1	78.50
			3	78.64
			5	78.66
			7	77.47
			9	<b>79.16</b>
			11	78.74
			13	78.35
			15	78.54

Table 2: **Performance comparison under different distribution numbers.** Num represents the number of distributions per class.

improvements while class global consistency loss alone is 2.43% mIoU improvements. It seems that class local consistency loss is more important than class global consistency loss, as seen by the results. But the simultaneous use of two losses can bring 4% mIoU performance improvements. This shows that the two losses complement each other and together improve the performance of the segmentation.

**Coefficient  $\alpha$  and  $\beta$**  We set several different sets of hyper-parameters to compare the results. As illustrated in Table 4, the performance of the model is more sensitive to the values of  $\alpha$  and  $\beta$ . When  $\alpha$  is set to 0.01,  $\beta$  is set to 0.1, compare to 0.01, the difference in performance is approximately 0.9%. According to the results, we obtain the optimal pair of parameters, which  $\alpha$  is 0.01,  $\beta$  is 0.05. Similarly, we set such optimal parameter pairs in other comparative experiments.

**Visualization results with Baseline** We integrated MDRL into the FCN network and obtained the segmentation results. As shown in Figure 4, compare with FCN, our method appears to be superior.

BaseLine	$L_{clcl}$	$L_{cgcl}$	mIoU
✓			75.16
✓	✓		78.20
✓		✓	77.59
✓	✓	✓	<b>79.16</b>

Table 3: **Validate the validity of the class local consistency loss and class global consistency loss respectively.** The results of this experiment are obtained by training the ResNet50-based FCN network on the Cityscapes dataset.

## 4.3. Comparison with State-of-the-Art

**Results on ADE20K** The results with other state-of-the-art methods on ADE20K dataset are summarized in Table 5. Integration of MDRL into PSPNet[42] with ResNet101 as backbone resulted in 3.41% mIoU im-

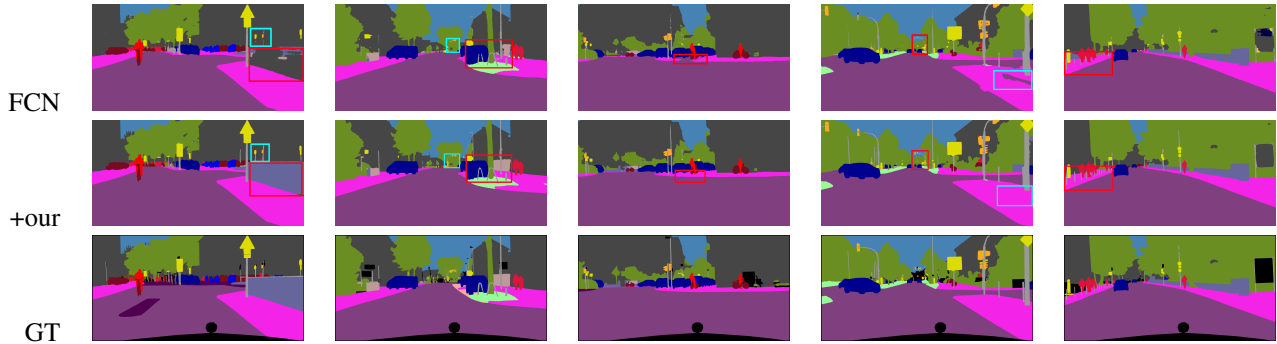


Figure 4: **Visual comparisons with FCN and FCN+MDRL on the validation set of Cityscapes.**The last line indicates the ground-truth.

$\alpha$	$\beta$	mIoU
0.01	0.01	78.97
	0.02	78.8
	0.03	78.00
	0.05	<b>79.16</b>
	0.06	78.51
	0.07	78.03
	0.1	78.07
	0.45	78.58
0.02	0.01	78.36

Table 4: **Ablation experiments of class local consistency loss and global consistency loss weights.** The results of this experiment are obtained by training the ResNet50-based FCN network on the Cityscapes dataset with different  $\alpha$  and  $\beta$ .

improvements under multi-scale and flipping test. Under ResNet-101, our method achieve a mIoU of 46.7%, which is 0.8%,0.94%,1.2% mIoU higher than ACNet[12],CCNet[16],DMNet[13]. Besides, under the setting of PSPNet as the semantic aggregation network, MRDL outperforms previous best method MCIBI++ by 0.71%/0.64% mIoU improvements when ResNet-50/ResNet-101 as backbone. These results show that it is more efficient to use multiple distribution features to describe the intra-class variations.

**Results on Cityscapes** As shown in Table 6, we also compared the performance with other state-of-the-art methods on the validation set of Cityscapes. The experimental results in the table are all based on single scale testing. Under ResNet-101 as backbone, Integration of MDRL into PSPNet[42] resulted in 1.25% mIoU improvements. Meanwhile, compare with other state-of-the-art methods, our method outperforms DNL[35],OCRNet[37],ISNet[19] by 0.61%,0.31%,0.45% mIoU. Besides, our method is 0.93%

Method	Backbone	Stride	mIoU
OCNet[38]	ResNet-101	8x	45.45
CCNet[16]	ResNet-101	8x	45.76
ACNet[12]	ResNet-101	8x	45.90
DMNet[13]	ResNet-101	8x	45.50
EncNet[40]	ResNet-101	8x	44.65
PSPNet[42]	ResNet-101	8x	43.29
PSANet[43]	ResNet-101	8x	43.77
APCNet[14]	ResNet-101	8x	45.38
OCRNet[37]	ResNet-101	8x	45.28
PSPNet[42]	ResNet-269	8x	44.94
UperNet[33]	ResNet-101	8x	44.85
PSPNet+MCIBI++[20]‡	ResNet-50	8x	44.72
PSPNet+MCIBI++[20]‡	ResNet-101	8x	46.06
PSPNet+MDRL	ResNet-50	8x	<b>45.43</b>
PSPNet+MDRL	ResNet-101	8x	<b>46.70</b>

Table 5: **Segmentation results on ADE20K validation set with other state-of-the-art methods.** Multi-scale and flipping testing are adopted for fair comparison. ‡means that this is our re-implemented result under the same experimental setting.

higher than MCIBI[18] based on ResNet-50 and 0.52% higher than MCIBI++[20] when ResNet-101 as backbone.

**Qualitative Results with State-of-the-Arts** We compared the visualization results with the state-of-the-arts method MCIBI++[20] under the same conditions. As shown in Figure 5. Our method performs better between individuals belonging to the same class with large differences. For example, the brightness of the road in the first row is different. Pedestrians located on the right side of the street wearing with different colors and different brightness in the second row. The third row of cars with different colors. The fourth line of indoor scenes with different brightness and colors of chandelier and people. The results show that our method is

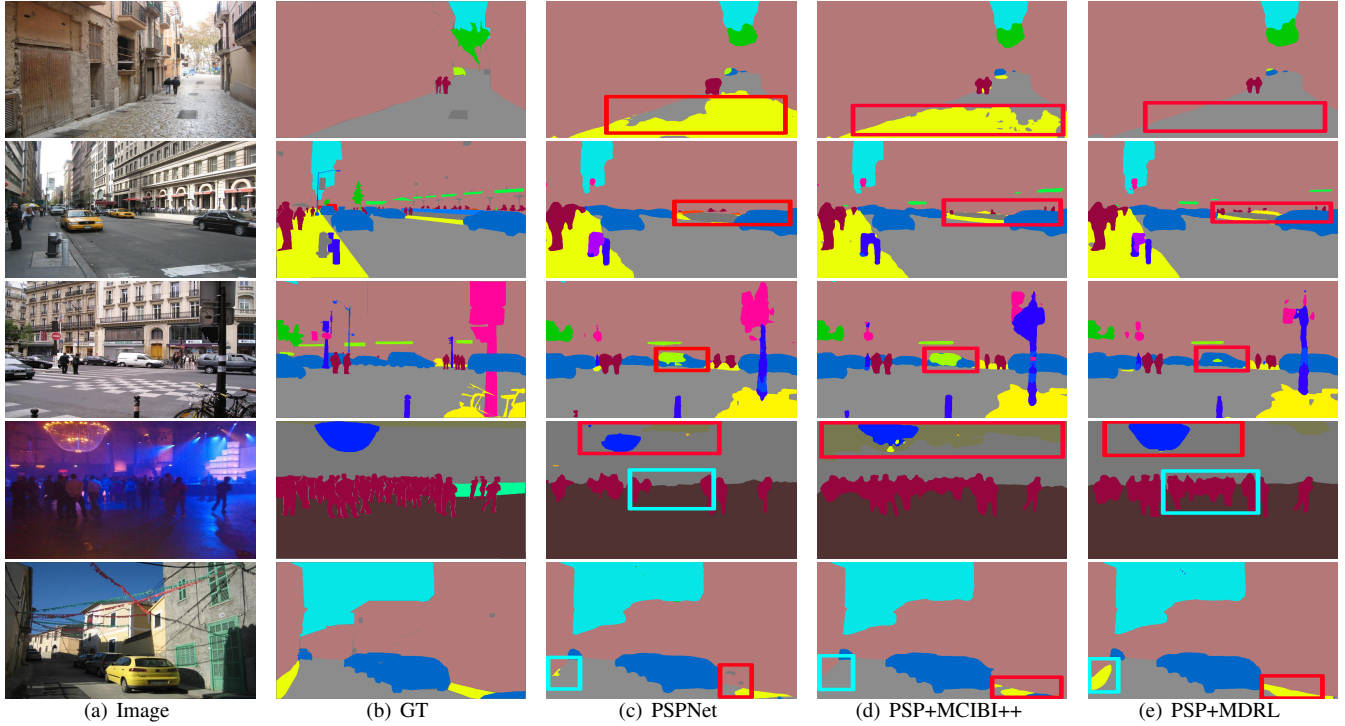


Figure 5: **Qualitative results on the validation set of ADE20K.** All models here are trained with ResNet-50 as backbone under the same setting.

Method	Backbone	Stride	mIoU
GCNet[2]	ResNet-101	8x	79.03
PSANet[43]	ResNet-101	8x	79.31
ANN[47]	ResNet-101	8x	77.14
NonLocal[31]	ResNet-101	8x	78.93
CCNet[16]	ResNet-101	8x	78.87
EncNet[40]	ResNet-101	8x	78.55
DANet[11]	ResNet-101	8x	80.41
DNL[35]	ResNet-101	8x	80.41
OCRNet[37]	ResNet-101	8x	80.70
PSPNet[42]	ResNet-101	8x	79.76
ISNet[19]	ResNet-50	8x	79.32
ISNet[19]	ResNet-101	8x	80.56
PSPNet+MCIBI[18]‡	ResNet-50	8x	79.12
PSPNet+MCIBI++[20]‡	ResNet-101	8x	80.49
PSPNet+MDRL	ResNet-50	8x	<b>80.05</b>
PSPNet+MDRL	ResNet-101	8x	<b>81.01</b>

Table 6: **Segmentation results on Cityscapes validation set with other state-of-the-art methods.** Only single-scale testing is adopted here. ‡means that this is our implemented result under the same experimental setting.

excellent in segmenting objects belonging to the same class with large differences. Besides, the result in the fifth row shows that our method can better identify two objects that are similar, but belong to different classes. Qualitative results show the importance of using multiple distributions to describe intra-class variations.

## 5. Conclusion

This paper presents a new perspective to describe class representation for semantic segmentation. We introduce the multiple distributions to describe intra-class variations. Then, we propose multiple distributions representation learning to augment the pixel representations. The class multiple distributions consistency strategy is committed to generating class-level multiple distribution features, more fine-grained multiple distribution feature representations are obtained through the feature voting and multi-distribution semantic aggregation module. Qualitative Results demonstrate that our method performs better in classifying objects of the same class but with large differences and objects of different classes but similar. Experimental results show that our approach can be integrated into existing popular segmentation frameworks and achieve good performance. Meanwhile, our method achieved the state-of-the-art performance on two challenging datasets.



## References

- [1] Inigo Alonso, Alberto Sabater, David Ferstl, Luis Monteseano, and Ana C Murillo. Semi-supervised semantic segmentation with pixel-level contrastive learning from a class-wise memory bank. In *Proceedings of the IEEE/CVF International Conference on Computer Vision*, pages 8219–8228, 2021.
- [2] Yue Cao, Jiarui Xu, Stephen Lin, Fangyun Wei, and Han Hu. Gcnet: Non-local networks meet squeeze-excitation networks and beyond. In *Proceedings of the IEEE/CVF international conference on computer vision workshops*, pages 0–0, 2019.
- [3] Mathilde Caron, Ishan Misra, Julien Mairal, Priya Goyal, Piotr Bojanowski, and Armand Joulin. Unsupervised learning of visual features by contrasting cluster assignments. *Advances in neural information processing systems*, 33:9912–9924, 2020.
- [4] Liang-Chieh Chen, George Papandreou, Iasonas Kokkinos, Kevin Murphy, and Alan L Yuille. Deeplab: Semantic image segmentation with deep convolutional nets, atrous convolution, and fully connected crfs. *IEEE transactions on pattern analysis and machine intelligence*, 40(4):834–848, 2017.
- [5] Liang-Chieh Chen, George Papandreou, Florian Schroff, and Hartwig Adam. Rethinking atrous convolution for semantic image segmentation. *arXiv preprint arXiv:1706.05587*, 2017.
- [6] Liang-Chieh Chen, Yukun Zhu, George Papandreou, Florian Schroff, and Hartwig Adam. Encoder-decoder with atrous separable convolution for semantic image segmentation. In *Proceedings of the European conference on computer vision (ECCV)*, pages 801–818, 2018.
- [7] Yihong Chen, Yue Cao, Han Hu, and Liwei Wang. Memory enhanced global-local aggregation for video object detection. In *Proceedings of the IEEE/CVF conference on computer vision and pattern recognition*, pages 10337–10346, 2020.
- [8] Marius Cordts, Mohamed Omran, Sebastian Ramos, Timo Rehfeld, Markus Enzweiler, Rodrigo Benenson, Uwe Franke, Stefan Roth, and Bernt Schiele. The cityscapes dataset for semantic urban scene understanding. In *Proceedings of the IEEE conference on computer vision and pattern recognition*, pages 3213–3223, 2016.
- [9] Marco Cuturi. Sinkhorn distances: Lightspeed computation of optimal transport. *Advances in neural information processing systems*, 26, 2013.
- [10] Jia Deng, Wei Dong, Richard Socher, Li-Jia Li, Kai Li, and Li Fei-Fei. Imagenet: A large-scale hierarchical image database. In *2009 IEEE conference on computer vision and pattern recognition*, pages 248–255. Ieee, 2009.
- [11] Jun Fu, Jing Liu, Haijie Tian, Yong Li, Yongjun Bao, Zhiwei Fang, and Hanqing Lu. Dual attention network for scene segmentation. In *Proceedings of the IEEE/CVF conference on computer vision and pattern recognition*, pages 3146–3154, 2019.
- [12] Jun Fu, Jing Liu, Yuhang Wang, Yong Li, Yongjun Bao, Jinhui Tang, and Hanqing Lu. Adaptive context network for scene parsing. In *Proceedings of the IEEE/CVF International Conference on Computer Vision*, pages 6748–6757, 2019.
- [13] Junjun He, Zhongying Deng, and Yu Qiao. Dynamic multi-scale filters for semantic segmentation. In *Proceedings of the IEEE/CVF International Conference on Computer Vision*, pages 3562–3572, 2019.
- [14] Junjun He, Zhongying Deng, Lei Zhou, Yali Wang, and Yu Qiao. Adaptive pyramid context network for semantic segmentation. In *Proceedings of the IEEE/CVF Conference on Computer Vision and Pattern Recognition*, pages 7519–7528, 2019.
- [15] Kaiming He, Xiangyu Zhang, Shaoqing Ren, and Jian Sun. Deep residual learning for image recognition. In *Proceedings of the IEEE conference on computer vision and pattern recognition*, pages 770–778, 2016.
- [16] Zilong Huang, Xinggang Wang, Lichao Huang, Chang Huang, Yunhao Wei, and Wenyu Liu. Ccnet: Criss-cross attention for semantic segmentation. In *Proceedings of the IEEE/CVF international conference on computer vision*, pages 603–612, 2019.
- [17] Xu Ji, Joao F Henriques, and Andrea Vedaldi. Invariant information clustering for unsupervised image classification and segmentation. In *Proceedings of the IEEE/CVF International Conference on Computer Vision*, pages 9865–9874, 2019.
- [18] Zhenchao Jin, Tao Gong, Dongdong Yu, Qi Chu, Jian Wang, Changhu Wang, and Jie Shao. Mining contextual information beyond image for semantic segmentation. In *Proceedings of the IEEE/CVF International Conference on Computer Vision*, pages 7231–7241, 2021.
- [19] Zhenchao Jin, Bin Liu, Qi Chu, and Nenghai Yu. Isnet: Integrate image-level and semantic-level context for semantic segmentation. In *Proceedings of the IEEE/CVF International Conference on Computer Vision*, pages 7189–7198, 2021.
- [20] Zhenchao Jin, Dongdong Yu, Zehuan Yuan, and Lequan Yu. Mcibi++: Soft mining contextual information beyond image for semantic segmentation. *IEEE Transactions on Pattern Analysis and Machine Intelligence*, 2022.
- [21] Alexander Kirillov, Ross Girshick, Kaiming He, and Piotr Dollár. Panoptic feature pyramid networks. In *Proceedings of the IEEE/CVF conference on computer vision and pattern recognition*, pages 6399–6408, 2019.
- [22] Suichan Li, Dapeng Chen, Bin Liu, Nenghai Yu, and Rui Zhao. Memory-based neighbourhood embedding for visual recognition. In *Proceedings of the IEEE/CVF International Conference on Computer Vision*, pages 6102–6111, 2019.
- [23] Xia Li, Zhisheng Zhong, Jianlong Wu, Yibo Yang, Zhouchen Lin, and Hong Liu. Expectation-maximization attention networks for semantic segmentation. In *Proceedings of the IEEE/CVF International Conference on Computer Vision*, pages 9167–9176, 2019.

- [24] Shikun Liu, Shuaifeng Zhi, Edward Johns, and Andrew J Davison. Bootstrapping semantic segmentation with regional contrast. *arXiv preprint arXiv:2104.04465*, 2021.
- [25] Wei Liu, Andrew Rabinovich, and Alexander C Berg. Parsenet: Looking wider to see better. *arXiv preprint arXiv:1506.04579*, 2015.
- [26] Ziwei Liu, Xiao Xiao Li, Ping Luo, Chen Change Loy, and Xiaoou Tang. Deep learning markov random field for semantic segmentation. *IEEE transactions on pattern analysis and machine intelligence*, 40(8):1814–1828, 2017.
- [27] Jonathan Long, Evan Shelhamer, and Trevor Darrell. Fully convolutional networks for semantic segmentation. In *Proceedings of the IEEE conference on computer vision and pattern recognition*, pages 3431–3440, 2015.
- [28] Tao Ruan, Ting Liu, Zilong Huang, Yunchao Wei, Shikui Wei, and Yao Zhao. Devil in the details: Towards accurate single and multiple human parsing. In *Proceedings of the AAAI conference on artificial intelligence*, volume 33, pages 4814–4821, 2019.
- [29] Jingdong Wang, Ke Sun, Tianheng Cheng, Borui Jiang, Chaorui Deng, Yang Zhao, Dong Liu, Yadong Mu, Mingkui Tan, Xinggang Wang, et al. Deep high-resolution representation learning for visual recognition. *IEEE transactions on pattern analysis and machine intelligence*, 43(10):3349–3364, 2020.
- [30] Wenguan Wang, Tianfei Zhou, Fisher Yu, Jifeng Dai, Ender Konukoglu, and Luc Van Gool. Exploring cross-image pixel contrast for semantic segmentation. In *Proceedings of the IEEE/CVF International Conference on Computer Vision*, pages 7303–7313, 2021.
- [31] Xiaolong Wang, Ross Girshick, Abhinav Gupta, and Kaiming He. Non-local neural networks. In *Proceedings of the IEEE conference on computer vision and pattern recognition*, pages 7794–7803, 2018.
- [32] Yuchao Wang, Haochen Wang, Yujun Shen, Jingjing Fei, Wei Li, Guoqiang Jin, Liwei Wu, Rui Zhao, and Xinyi Le. Semi-supervised semantic segmentation using unreliable pseudo-labels. In *Proceedings of the IEEE/CVF Conference on Computer Vision and Pattern Recognition*, pages 4248–4257, 2022.
- [33] Tete Xiao, Yingcheng Liu, Bolei Zhou, Yuning Jiang, and Jian Sun. Unified perceptual parsing for scene understanding. In *Proceedings of the European conference on computer vision (ECCV)*, pages 418–434, 2018.
- [34] Maoke Yang, Kun Yu, Chi Zhang, Zhiwei Li, and Kuiyuan Yang. Denseaspp for semantic segmentation in street scenes. In *Proceedings of the IEEE conference on computer vision and pattern recognition*, pages 3684–3692, 2018.
- [35] Minghao Yin, Zhuliang Yao, Yue Cao, Xiu Li, Zheng Zhang, Stephen Lin, and Han Hu. Disentangled non-local neural networks. In *Computer Vision—ECCV 2020: 16th European Conference, Glasgow, UK, August 23–28, 2020, Proceedings, Part XV 16*, pages 191–207. Springer, 2020.
- [36] Fisher Yu, Vladlen Koltun, and Thomas Funkhouser. Dilated residual networks. In *Proceedings of the IEEE conference on computer vision and pattern recognition*, pages 472–480, 2017.
- [37] Yuhui Yuan, Xilin Chen, and Jingdong Wang. Object-contextual representations for semantic segmentation. In *Computer Vision—ECCV 2020: 16th European Conference, Glasgow, UK, August 23–28, 2020, Proceedings, Part VI 16*, pages 173–190. Springer, 2020.
- [38] Yuhui Yuan, Lang Huang, Jianyuan Guo, Chao Zhang, Xilin Chen, and Jingdong Wang. Ocnet: Object context network for scene parsing. *arXiv preprint arXiv:1809.00916*, 2018.
- [39] Fan Zhang, Yanqin Chen, Zhihang Li, Zhibin Hong, Jingtuo Liu, Feifei Ma, Junyu Han, and Errui Ding. Acfnet: Attentional class feature network for semantic segmentation. In *Proceedings of the IEEE/CVF International Conference on Computer Vision*, pages 6798–6807, 2019.
- [40] Hang Zhang, Kristin Dana, Jianping Shi, Zhongyue Zhang, Xiaoang Wang, Amrith Tyagi, and Amit Agrawal. Context encoding for semantic segmentation. In *Proceedings of the IEEE conference on Computer Vision and Pattern Recognition*, pages 7151–7160, 2018.
- [41] Hang Zhang, Chongruo Wu, Zhongyue Zhang, Yi Zhu, Haibin Lin, Zhi Zhang, Yue Sun, Tong He, Jonas Mueller, R Manmatha, et al. Resnest: Split-attention networks. In *Proceedings of the IEEE/CVF Conference on Computer Vision and Pattern Recognition*, pages 2736–2746, 2022.
- [42] Hengshuang Zhao, Jianping Shi, Xiaojuan Qi, Xiaoang Wang, and Jiaya Jia. Pyramid scene parsing network. In *Proceedings of the IEEE conference on computer vision and pattern recognition*, pages 2881–2890, 2017.
- [43] Hengshuang Zhao, Yi Zhang, Shu Liu, Jianping Shi, Chen Change Loy, Dahua Lin, and Jiaya Jia. Pscanet: Pointwise spatial attention network for scene parsing. In *Proceedings of the European conference on computer vision (ECCV)*, pages 267–283, 2018.
- [44] Shuai Zheng, Sadeep Jayasumana, Bernardino Romera-Paredes, Vibhav Vineet, Zhizhong Su, Dalong Du, Chang Huang, and Philip HS Torr. Conditional random fields as recurrent neural networks. In *Proceedings of the IEEE international conference on computer vision*, pages 1529–1537, 2015.
- [45] Bolei Zhou, Hang Zhao, Xavier Puig, Sanja Fidler, Adela Barriuso, and Antonio Torralba. Scene parsing through ade20k dataset. In *Proceedings of the IEEE conference on computer vision and pattern recognition*, pages 633–641, 2017.
- [46] Tianfei Zhou, Wenguan Wang, Ender Konukoglu, and Luc Van Gool. Rethinking semantic segmentation: A prototype view. In *Proceedings of the IEEE/CVF Conference on Computer Vision and Pattern Recognition*, pages 2582–2593, 2022.
- [47] Zhen Zhu, Mengde Xu, Song Bai, Teng Teng Huang, and Xi-ang Bai. Asymmetric non-local neural networks for seman-

tic segmentation. In *Proceedings of the IEEE/CVF International Conference on Computer Vision*, pages 593–602, 2019.